Hindawi Publishing Corporation
Journal of Biomedicine and Biotechnology
Volume 2007, Article ID 76514, 9 pages
doi:10.1155/2007/76514

Research Article

Imaging $GABA_c$ Receptors with Ligand-Conjugated Quantum Dots

Ian D. Tomlinson,[1] Hélène A. Gussin,[2] Deborah M. Little,[2,3] Michael R. Warnement,[1] Haohua Qian,[2] David R. Pepperberg,[2] and Sandra J. Rosenthal[1]

[1] *Department of Chemistry, Vanderbilt University, Station B 311822, Nashville, TN 37235, USA*
[2] *Lions of Illinois Eye Research Institute, Department of Ophthalmology and Visual Sciences, University of Illinois at Chicago, Chicago, IL 60612, USA*
[3] *Department of Neurology and Rehabilitation, University of Illinois at Chicago, Chicago, IL 60612, USA*

Correspondence should be addressed to Sandra J. Rosenthal, sandra.j.rosenthal@vanderbilt.edu

Received 14 May 2007; Revised 30 August 2007; Accepted 21 December 2007

Recommended by Marek Osinski

We report a methodology for labeling the GABAc receptor on the surface membrane of intact cells. This work builds upon our earlier work with serotonin-conjugated quantum dots and our studies with PEGylated quantum dots to reduce nonspecific binding. In the current approach, a PEGylated derivative of muscimol was synthesized and attached via an amide linkage to quantum dots coated in an amphiphilic polymer derivative of a modified polyacrylamide. These conjugates were used to image $GABA_C$ receptors heterologously expressed in Xenopus laevis oocytes.

1. INTRODUCTION

Quantum dots (qdots) are nanometer-sized semiconductor crystals that have unique physical properties that differ from bulk material. The fluorescent properties of qdots have been widely described, and numerous applications based upon these fluorescent properties have been reported. In addition, previous studies have reported the properties of many varieties of qdots [1–8]. Of these, the most widely studied are cadmium selenide/zinc sulfide core-shell nanocrystals. These consist of a semiconductor core of cadmium selenide encapsulated in a multilayer shell of zinc sulfide doped with cadmium [9]. The shell passivates the surface of the core, and the band gap is wider than that of the core, enabling quantum confinement of an electron-hole pair generated in the core after photoexcitation. Ultimately, the electron hole pair recombines, resulting in a fluorescent emission of a lower-energy photon in the visible region of the spectrum [10]. The energy of the emitted photon is determined by the size of the quantum confinement (or the size of the qdot). Smaller qdots emit blue light and larger ones emit red light. Qdots have several advantages over conventional fluorescent dyes; these include increased photostability, increased brightness, quantum yields in excess of 80–90% [1, 9, 11], and a narrow emission spectrum (less than 30 nm full width at half-maximum in commercial products) [12–15]. Furthermore, their multivalent surfaces enable the attachment of more than one type of ligand or multiple copies of a ligand to a single qdot.

Since their introduction into biology as imaging agents in 1998 [16, 17], qdots have increasingly found applications as fluorescent probes in biology. To be useful as fluorescent probes in biological systems, qdots must be soluble in water and commonly used buffers. Additionally, they must have colloidal stability and low nonspecific adsorption to cellular membranes. These properties have been achieved using a number of techniques, including encapsulation in micelles [18], silanization [19], encapsulation in amphiphilic polymers [20, 21], and encapsulation in proteins such as streptavidin [22]. To further reduce nonspecific adsorption to cellular membranes, a number of techniques may be used to modify the surface chemistry of qdots. For example, we have recently demonstrated that nonspecific binding can be significantly reduced by attaching polyethylene glycol chains (i.e., by PEGylating) qdots coated in an amphiphilic modified polyacrylic acid polymer (AMP) [23]. The length of the PEG chain and the PEG loading were demonstrated to be important in reducing nonspecific adsorption to cellular

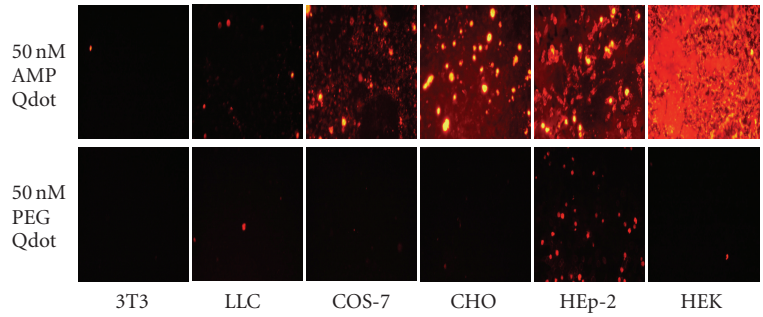

Figure 1: A comparison of nonspecific adsorption of AMP-coated qdots to the surfaces of 6 different cell types. These experiments employed AMP-coated qdots that were either unconjugated (upper row) or conjugated to PEG2000 (lower row).

membranes. When PEGs with short (less than 12) repeat units were conjugated to qdots, a small reduction in nonspecific adsorption to cellular membranes was observed. This reduction increased in magnitude when larger PEGs were used. Figure 1 shows the effects of PEGylation (PEG2000) on nonspecific adsorption to 6 different cell types. These cells were treated with a 50 nM solution of PEGylated AMP-coated qdots or a 50 nM solution of AMP-coated qdots. A significant reduction in nonspecific adsorption to cellular membranes was obtained by the addition of PEG2000. The nonspecific adsorption is cell-type specific, as can be seen in the relatively low nonspecific adsorption of AMP-coated qdots to the surfaces of 3T3 cells compared to the high levels of nonspecific adsorption to HEK cells.

In addition to surface modification techniques such as PEGylation, a wide variety of biologically active molecules have been attached to qdots, including proteins [24–31], peptides [32–34], DNA [35–43], RNA [44], peptide nucleic acid (PNA) [45], cytokines [46], viruses [47], and antibodies [48–54]. The qdots-based imaging applications that have been reported in the literature are extensive and encompass a wide variety of imaging applications. Of these, live cell imaging [51] and whole animal imaging [52] have received a great deal of interest. In addition to qdots that emit in the visible region of the electromagnetic spectrum, near-infrared qdots have been developed that have a cadmium telluride core instead of a cadmium selenide core. These near-IR dots have found applications in the clinic as tools for imaging sentinel lymph nodes during surgery [53].

Our research efforts focus on the central nervous system. We are interested in using qdots that have been conjugated with small molecules [55–60], antibodies [61], and peptides [34] to image receptors and transporters in cell cultures, oocytes, and, ultimately, neurons. In our early work, we used qdots to image the serotonin transporter (SERT) using PEGylated serotonin ligands [62] attached to the surfaces of qdots via an acid-base interaction (see Figure 2). These conjugates antagonized the serotonin transporter protein (SERT) with an IC_{50} of 115 μM in transfected HEK-293 cells. Using these conjugates we were able to image SERT expressed in HEK-293 cells [55].

Numerous biofunctionalization methods for qdots have been reported in recent years. Qdot preparations that contain an amphiphilic coating on the qdots surface are commercially available, and a variety of methodologies, including those involving sulfo-SMCC [63] and adaptor proteins [64], have been used to conjugate ligands to the coated qdot. Our current strategy uses commercially available qdots that have either an amphiphilic coating (AMP) on the surface of the dots, or AMP qdots with an additional coating of streptavidin. PEGylated ligands may be attached to the surface of these dots using two different methodologies. Either they may be covalently attached to the AMP coating using 1-[3-(dimethylamino)propyl]-3-ethylcarbodiimide hydrochloride (EDC) coupling chemistry, or a biotinylated derivative of the biologically active ligand may be attached to the surface of streptavidin-coated qdots via a streptavidin-biotin interaction. Using the PEGylated ligand approach, we have synthesized a novel qdot conjugate and tested its binding activity to the $GABA_C$ receptor, a ligand-gated ion channel that is found in retina and other central nervous system tissue and that is activated in vivo by γ-aminobutyric acid (GABA). Specifically, we have investigated a PEG derivative of muscimol, a known agonist of both $GABA_C$ and $GABA_A$ receptors (see Figure 3). Multiple copies of this ligand have been conjugated to the surface of AMP-coated qdots and used to image $GABA_C$ receptors expressed in *Xenopus laevis* oocytes [65].

2. METHODOLOGY

Streptavidin-coated qdots and AMP-coated qdots with maximum emissions of 605 and 585 nm were obtained from Invitrogen (Carlsbad, Calif, USA). *N*-Hydroxy urea, dimethyl acetylenedicarboxylate, 1,5-diazabicyclo[5.4.0] undec-7-ene (DBU), borane dimethyl sulfide, and *N*-hydroxy succinimide (NHS) were obtained from Sigma-Aldrich (St.Louis, Mo, USA). Trifluoroacetic acid (TFA), potassium hydroxide, and hydrazine monohydrate were obtained from VWR (West Chester, Pa, USA). All reagents were used without further purification. Borate buffer was obtained from PolySciences, Inc. (Warrington, Pa, USA), and Sephadex G-50 was obtained from Amersham Biosciences (Uppsala, Sweden). *t*-Butyloxacarbamate (BOC)-protected *N*-hydroxy succinimide-activated PEG3400 ester (BOC-PEG-NHS) was obtained from Nektar Therapeutics (Huntsville, Ala, USA).

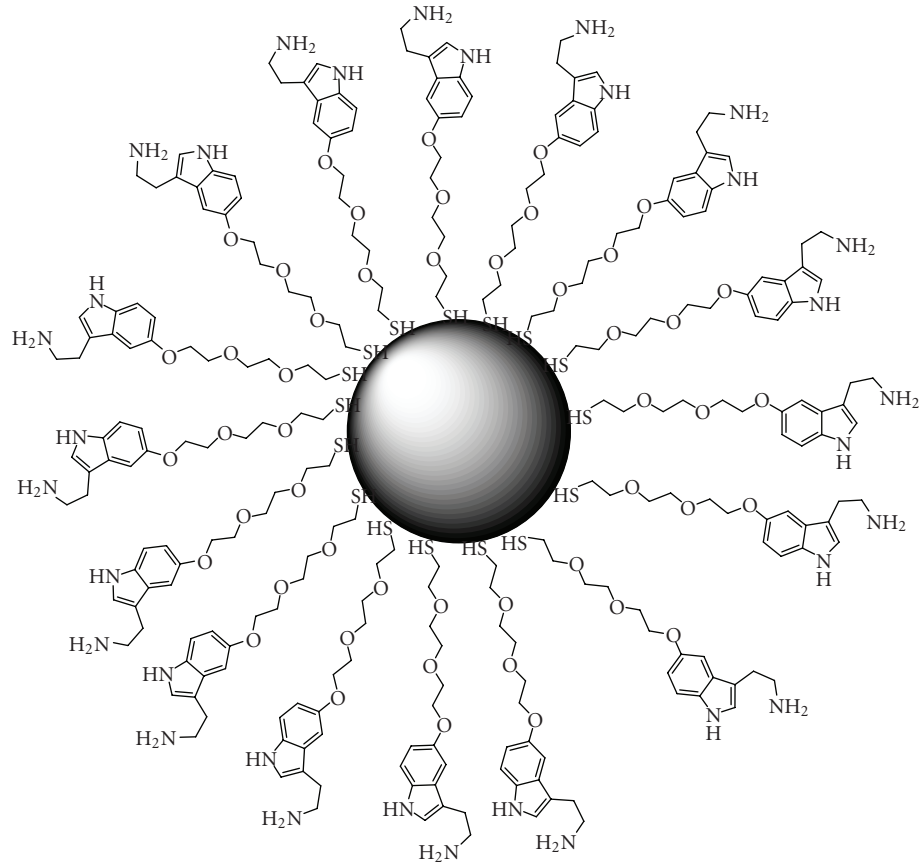

Figure 2: Serotonin-coated qdots used to label SERT-expressing cells.

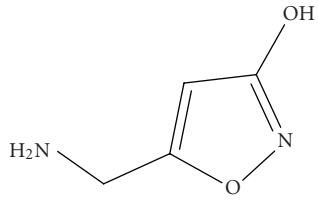

Muscimol

Figure 3: Muscimol, a $GABA_C$ and $GABA_A$ receptor agonist.

2.1. Synthesis of the muscimol ligand

Muscimol was synthesized using the method described by Frey and Jäger [66]. This was then coupled to the PEG linker via an aminohexanoyl NHS ester to give the PEGylated muscimol ligand. The ligand was characterized by matrix-assisted laser desorption/ionization time-of-flight (MALDI-TOF) mass spectroscopy and conjugated to AMP-coated qdots via an EDC coupling.

2.1.1. Muscimol synthesis

Muscimol was synthesized using the synthetic methodology shown in Scheme 1. Dimethyl acetylenedicarboxylate (3.1 mL) was added dropwise to a solution of *N*-hydroxy urea (1.9 g, 25 mmols) and DBU (4.19 g, 28 mmols) in methanol (25 mL) at 0°C. The resulting solution was stirred at 0°C for 10 minutes, and then evaporated under reduced pressure. Concentrated hydrochloric acid was added until a pH of 1 was obtained. This solution was extracted with diethyl ether, dried over magnesium sulfate, filtered, and then evaporated. The resulting solid was recrystallized from methylene chloride to yield 1.1 g of methyl 3-hydroxy isoxazole-5-carboxylate (I) in a 32% yield. This was converted to (II) by stirring 0.84 g of (I) in ammonium hydroxide (3 mL) and methanol (3 mL) for 1 hour, followed by recrystallization from ethanol to give 0.75 g of 3-hydroxyisoxazole-5-carboxamide (II) in 88% yield as the ammonium salt. Muscimol (III) was obtained from 1 g of (II) by reduction with borane dimethyl sulfide in tetrahydrofuran (THF) to give 0.2 g of (III) in a 22% yield after purification by ion exchange chromatography.

2.1.2. Synthesis of PEGylated muscimol ligand

The synthetic route used to synthesize the PEGylated muscimol ligand is shown in Scheme 2. Initially, the aminohexanoyl spacer was synthesized by reacting 6-amino hexanoic acid with ^{t}BOC anhydride in methanol to give 6-(*tert*-butoxycarbonylamino)hexanoic acid (IV) in a 58% yield. This was converted to 2,5-dioxopyrrolidin-1-yl

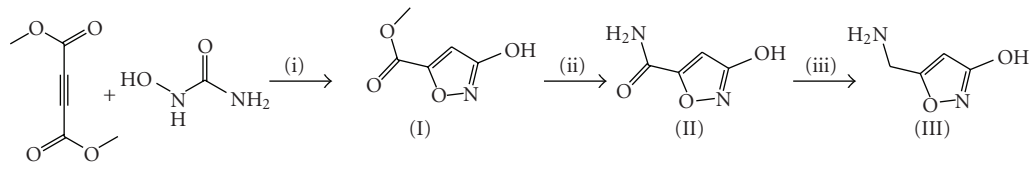

Scheme 1: Synthesis of Muscimol: (i) DBU, (ii) NH_3, and (iii) BH_3.

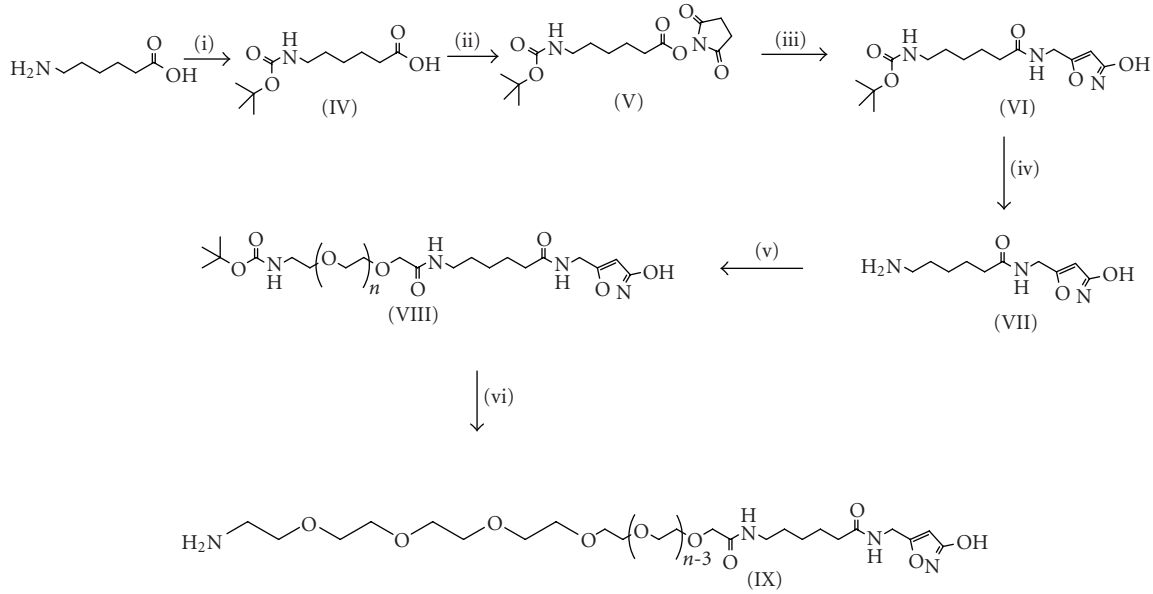

Scheme 2: Synthesis of muscimol ligand: (i) BOC anhydride, (ii) NHS, DCC, (iii) Muscimol, (iv) TFA,(v) BOC-PEG3400-NHS, and (vi) TFA.

6-(*tert*-butoxycarbonylamino)hexanoate (V) by reacting (IV) with NHS in the presence of dicyclo carbodiimide (DCC). The product was recrystallized from ether/hexanes resulting in a 38% yield of (V). This was coupled to muscimol in pyridine to give *tert*-butyl 6-((3-hydroxyisoxazol-5-yl)methylamino)-6-oxahexylcarbamate (VI) in a 54% yield. The BOC protecting group was removed using TFA to give 6-amino-*N*-((3-hydroxyisoxazol-5-yl)methyl)hexanamide (VII) in a 100% yield. This was coupled to ^{t}BOC protected PEG3400 NHS ester to give (VIII) in 100% yield. The BOC protecting group was removed using TFA to give (IX).

2.1.3. MALDI-TOF mass spectroscopy

Compounds (VIII) and (IX) were characterized by MALDI-TOF mass spectroscopy (Applied Biosystems Voyager mass spectrometer equipped with a 337 nm nitrogen laser) using an acceleration voltage of 25 kV, and the spectra were obtained by averaging of 30–64 scans [65]. The samples were prepared using a saturated matrix stock solution, consisting of 2,5-dihydroxybenzoic acid and 0.01 M sodium iodide dissolved in methanol. The PEG derivatives (VIII) and (IX) were prepared (5 mM) in methanol. The sample was added to the matrix by mixing the sample and stock solutions in a 2 : 5 : 2 ratio of sample to matrix to salt (v/v). A 1-μL aliquot of each sample solution was placed on the sample plate. Mass calibration of the instrument employed a PEG standard, and was prepared using the same protocol as that employed for the other samples. Analysis of the resulting spectra indicated that compounds (VIII) and (IX) were polydisperse. Compound (VIII) exhibited masses ranging from 3241 Da to 4188 Da (indicative of muscimol conjugation to PEGs of different lengths), and a primary peak at 3726 Da. The treatment of (VIII) with TFA to yield compound (IX) resulted in a MALDI-TOF spectrum shift of 100 Da (primary peak at 3626 Da), consistent with loss of the BOC protecting group.

2.1.4. Ligand conjugation

The ligand was conjugated to qdots using an EDC coupling in which 1000 equivalents of ligand were mixed with 750 equivalents of NHS and EDC in borate buffer at pH 8.5. To this was added a solution of AMP-coated qdots (8.4 μM). This mixture was stirred for 1 hour at ambient temperature. Unbound ligand was removed by Sephadex G-50 chromatography. The coupling of amino-terminated PEG2000 to AMP-coated qdots using EDC has been studied in an earlier publication, and the efficiency of coupling has been reported to be ~20% when 2000 equivalents of methoxy-terminated

aminoPEG2000 are reacted with 1 equivalent of AMP-coated qdots [23]. Since the terminating muscimol of the present ligand is attached to PEG3400, the coupling efficiency is likely to be similar. On this basis, we estimate the number of muscimol ligands to be around 150–200 per qdot [65]. The derivatized qdots were characterized by electrophoresis in 1% agarose gel (see Figure 4). The gel demonstrates that the muscimol-conjugated qdots (Lane 3), as well as qdots conjugated with PEG2000 (Lane 4), have a wide distribution in the number of ligands attached to their surface, as they streak on the gel more than unconjugated qdots (Lane 2). It is important to note that mobility in the gel does not depend merely on mass, but rather on mass-to-charge ratio. Thus, despite the substantial difference in mass of the PEG2000 versus the muscimol-terminated PEG3400 ligand, the bands representing the qdots conjugates that contain (numerous copies of) these ligands exhibit similar mobilities (Lanes 3 and 4). The present experimental conditions (1% agarose gel) do not separate protein standards that span a molecular weight range of 10–250 kDa (data not shown).

2.2. Oocyte imaging

The oocytes used in this study were obtained from adult female *X. laevis* toads. The oocytes were stored in physiological saline (Ringer solution; 100 mM NaCl, 2 mM KCl, 2 mM $CaCl_2$, 1 mM $MgCl_2$, 10 mM glucose, and 5 mM HEPES, pH 7.4). Using previously reported procedures, we expressed $GABA_C$ receptors (human ρ1 and perch ρ1B) in *X. laevis* oocytes [67, 68]. cRNA (50 nL) for each of the receptor subunits was injected into the oocyte, and the oocytes were assayed after 18–72-hour incubation in Ringer solution containing 0.1 mg/mL gentamycin at 16–19°C to allow for expression of the $GABA_C$ receptors. Oocyte imaging was carried out in a glass-bottom dish into which $GABA_C$ expressing oocytes and oocytes that did not express $GABA_C$ were placed. These oocytes were incubated for 5–10 minutes in a drop ($\sim$25 μL) of solution containing either 34 nM AMP-coated qdots conjugated to the muscimol ligand, or 34 nM AMP-coated qdots that lacked conjugated muscimol ligand. The oocytes were then imaged using a confocal microscope (Leica model DM-IRE2 with 20x objective) with excitation at 476 nm, and with detection of fluorescence emission over a wavelength range (580–620 nm) that included the qdot emission peak (605 nm). At the beginning of experiments conducted on a given day, we established microscope settings relevant to excitation illumination and detection of fluorescence emission (gain and offset) with use of either a human ρ1 $GABA_C$-expressing or perch ρ1B $GABA_C$-expressing oocyte incubated with 34 nM muscimol-conjugated AMP-coated qdots. These settings were maintained without change for the entire day's measurements [65].

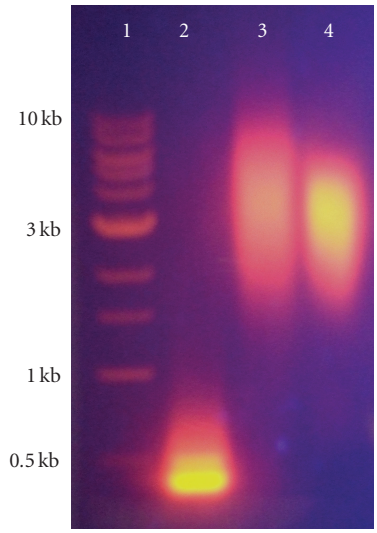

Figure 4: Agarose gel electrophoresis of qdots conjugates (1% agarose gel; Tris-acetate-EDTA buffer containing ethidium bromide for DNA visualization; 80 V potential difference). A 1-kb DNA ladder (Lane 1; New England Biolabs, Ipswich, Mass, USA), with DNA fragments ranging from 0.5–10 kilobases (kb) as indicated, was utilized to illustrate relative electrophoretic mobility of the qdot conjugates. Unconjugated AMP-coated qdots (Lane 2) have an increased mobility by comparison with both muscimol-conjugated qdots (Lane 3) and qdots conjugated with methoxy terminated PEG2000 (Lane 4), indicating successful functionalization of the qdot surface.

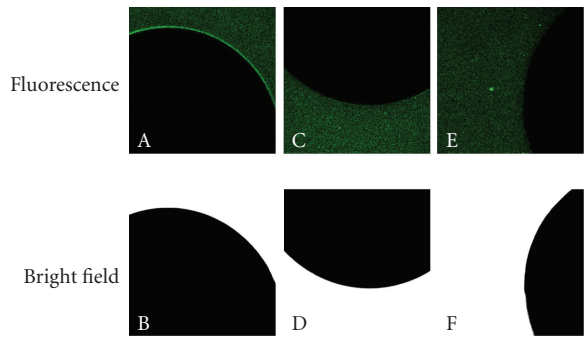

Figure 5: Fluorescence images (top row) and bright-field images (bottom row) of oocytes incubated with qdot-containing compounds for 10 minutes. The bright-field images illustrate the plane of focus of the opaque oocyte. Panels A and B show results from a human ρ1 $GABA_C$-expressing oocyte incubated with 34 nM muscimol-conjugated AMP-coated qdots. Panels C and D show a human ρ1 $GABA_C$-expressing oocyte incubated with a 34 nM solution of unconjugated AMP-coated qdots. Panels E and F show a nonexpressing oocyte incubated with 34 nM muscimol-conjugated AMP-coated qdots. Adapted from Gussin et al. [65].

3. RESULTS

3.1. Labeling of $GABA_C$-expressing oocytes with muscimol-conjugated qdots

Figure 5 shows the binding of muscimol-conjugated AMP-coated qdots and unconjugated AMP-coated qdots to oocytes expressing the human ρ1 $GABA_C$ receptor, and to non-expressing control oocytes (see Figure 5 legend). When $GABA_C$-expressing oocytes were incubated with a 34 nM solution of muscimol-conjugated dots for 10 minutes, a fluorescent halo was observed at the oocyte surface membrane

(panel A). The intensity of this halo exceeded that of the surrounding extracellular medium. The fluorescent image can be compared with the corresponding bright-field image (panel B), which shows the position and focus of the oocyte. By comparison with panel A, no fluorescence halo was observed upon similar incubation of a ρ1 $GABA_C$-expressing oocyte with AMP-coated qdots, that is, with a structure that lacked muscimol (panel C). Halo fluorescence of the oocyte surface membrane was also absent when a nonexpressing oocyte was incubated with 34 nM muscimol-conjugated dots (panel E). These results indicate that the muscimol ligand is necessary for binding of the conjugate to the oocyte surface membrane.

As noted in Section 2.1.4, the muscimol-conjugated AMP-coated qdot preparation used in the oocyte imaging experiments contained ~150–200 muscimol-terminated chains per qdot. In some preparations (not illustrated) of these muscimol-conjugated AMP-coated qdots, the extracellular medium surrounding the oocytes exhibited aggregation of the fluorescent particles. In developing the method of preparation of the conjugate, we observed that if 2000 equivalents of the muscimol ligand were reacted with AMP-coated qdots in the presence of 1500 equivalents of EDC and NHS, aggregates formed that subsequently precipitated from solution. It is likely that this aggregation is due to hydrogen bonding between muscimol ligands on adjacent qdots. The size and solubility of these aggregates likely depended on the number of ligands conjugated to the qdots.

3.2. Image analysis

To quantify the extent of binding of muscimol-conjugated AMP-coated qdots to the oocytes, we analyzed the surface membrane and extracellular regions of a given fluorescence image [65]. Using MetaMorph software (Offline Version 6.3r0; Universal Imaging Corp., Downington, Pa, USA), we determined the intensities of pixels underlying a multisegmented line that traced the arc-like border of the oocyte (15–25 straight-line segments; 450–750 pixels), and tabulated the resulting pixel values in relation to a 0–255 gray scale. We similarly determined the intensities of pixels that corresponded with an identical multisegment line constructed within the extracellular region of the image; tabulated intensities for this control extracellular region were taken as a measure of background (i.e., surround) fluorescence. For the image shown in Figure 5A, fluorescence intensities determined for the halo (henceforth termed "border") at the oocyte surface membrane and the surrounding extracellular medium (background) were 67.31 ± 36.79 (mean $\pm$ SD) and 22.30 ± 21.18, respectively. As reported by Gussin et al. [65], results obtained in experiments similar in design to that described in Figures 5A, 5B (human ρ1 $GABA_C$-expressing oocytes; incubation with 34 nM muscimol-conjugated dots) indicated a border fluorescence of 88.84 ± 64.84 and a background fluorescence of 31.60 ± 35.50 ($n = 11$), respectively. Additional experiments of the same design (not illustrated), conducted on oocytes expressing the perch ρ1B receptor [65], yielded border and background fluorescence intensities of 109.58 ± 58.42 and 18.54 ± 16.47 ($n = 4$), respectively. Aggregate results obtained in 4 experiments in which $GABA_C$-expressing oocytes were incubated with unconjugated AMP-coated qdots (see Figures 5C, 5D) yielded border and background fluorescence intensities of 15.79 ± 23.18 and 13.13 ± 18.17, respectively. Among 14 experiments that involved the incubation of 34 nM muscimol-conjugated dots with nonexpressing oocytes (see Figures 5E, 5F), border and background fluorescence intensities were 15.14 ± 22.35 and 16.78 ± 22.17, respectively, [65]. Two-way ANOVA analysis of results obtained with the muscimol-conjugated AMP-coated qdots showed that for both human ρ1 $GABA_C$-expressing and perch ρ1B $GABA_C$-expressing oocytes, the fluorescence intensity of the border differed significantly from that of the background. For nonexpressing oocytes incubated with the conjugate, there was no significant difference between border and background values. In addition, the treatment of $GABA_C$-expressing oocytes with free (i.e., non-qdot-conjugated) GABA, muscimol, or PEGylated muscimol significantly reduced binding of the muscimol-qdots conjugate to the oocyte surface membrane (see Gussin et al. [65] for further details).

4. DISCUSSION

The primary finding of the experiments involving the incubation of muscimol-conjugated AMP-coated qdots with $GABA_C$-expressing oocytes is that these conjugates exhibit specific binding at $GABA_C$ receptors. This binding depends on the presence of muscimol in the conjugate, as (unconjugated) AMP-coated qdots show no significant binding to oocytes expressing $GABA_C$ receptors. The approach described here builds on our earlier work with PEGylated serotonin attached to qdots in which we found that these conjugates exhibited binding at serotonin transporters expressed in HeLa and HEK cells. These findings indicate that it is possible to specifically label transporter proteins and ligand-gated receptors with qdots that have multiple copies of a membrane receptor or membrane transporter ligand attached through a PEG linker.

The presence of numerous copies of ligand in the muscimol-qdot conjugate described here raises the possibility that these conjugates bind to multiple $GABA_C$ receptors in a cross-linking fashion. Indeed, it is reasonable to hypothesize that the multiplicity of the muscimol ligand, as well as the length of the PEG linker that tethers each ligand to the qdot, favors such cross-linking. However, experiments conducted to date, while clearly establishing the ability of this conjugate to bind to cell-surface-expressed $GABA_C$ receptors, do not address the extent to which receptor cross-linking affects this binding activity. Other investigators have used fluorescent probes to track the diffusion dynamics of single receptors (single-particle tracking (SPT)), and such an SPT approach could be useful for evaluating the cross-linking activity of the present muscimol-qdot conjugate. For example, Dahan et al. [50] have examined the diffusion dynamics of glycine receptors in neuronal membranes by labeling the receptor with a conjugate consisting of a primary antireceptor antibody, biotinylated secondary antibody, and streptavidin-coated qdots. To test the extent

of receptor cross-linking by this conjugate, they investigated, as a comparison system, an Fab fragment of the primary antibody that had been linked to an organic fluorophore (Cy-3). Dahan et al. [50] found that the receptor dynamics determined with the qdot conjugate and the Cy-3-containing molecule were similar, indicating that neither the presence of the SA-qdots nor some other feature of the qdot-containing conjugate promoted significant receptor cross-linking. It should be emphasized that the structure of the presently described muscimol-qdot conjugate (see Figure 2) differs from the qdot-containing conjugate studied by Dahan et al. [50] in several respects, including the presence of a small-molecule ligand (muscimol) rather than an antibody as the receptor-reactive moiety, a high valency (copy number) of ligands per qdot, and a separation of each ligand from the qdot by a long linking chain (PEG3400). In future experiments, it may be possible to test for cross-linking by the muscimol-qdot conjugate using an approach in which $GABA_C$ receptor dynamics determined with the muscimol-qdots conjugate are compared with those determined using a structure optimized for SPT, for example, a fluorescent probe attached to a single receptor [26, 27].

ACKNOWLEDGMENTS

Liz Bentzen and David Wright assisted in the studies of nonspecific binding of qdots shown in this paper. The authors thank Niraj J. Muni for the helpful discussions. This research was supported by Grants EY016094, EY13693, EY05494, EY01792, EB003728, EM72048, and AG028662 from the National Institutes of Health, grants from the Daniel F. and Ada L. Rice Foundation (Skokie, Ill, USA), the American Health Assistance Foundation (Clarksburg, Md, USA), and the CINN Foundation (Chicago, Ill, USA), and an unrestricted departmental award from Research to Prevent Blindness (NewYork, NY, USA). Dr. Pepperberg is a Senior Scientific Investigator of Research to Prevent Blindness.

REFERENCES

[1] A. Watson, X. Wu, and M. Bruchez, "Lighting up cells with quantum dots," *BioTechniques*, vol. 34, no. 2, pp. 296–303, 2003.

[2] W. W. Yu, L. Qu, W. Guo, and X. Peng, "Experimental determination of the extinction coefficient of CdTe, CdSe, and CdS nanocrystals," *Chemistry of Materials*, vol. 15, no. 14, pp. 2854–2860, 2003.

[3] A. Striolo, J. Ward, J. M. Prausnitz, et al., "Molecular weight, osmotic second virial coefficient, and extinction coefficient of colloidal CdSe nanocrystals," *Journal of Physical Chemistry B*, vol. 106, no. 21, pp. 5500–5505, 2002.

[4] J. M. Tsay, M. Pflughoefft, L. A. Bentolila, and S. Weiss, "Hybrid approach to the synthesis of highly luminescent CdTe/ZnS and CdHgTe/ZnS nanocrystals," *Journal of the American Chemical Society*, vol. 126, no. 7, pp. 1926–1927, 2004.

[5] J. Zheng, J. T. Petty, and R. M. Dickson, "High quantum yield blue emission from water-soluble Au_8 nanodots," *Journal of the American Chemical Society*, vol. 125, no. 26, pp. 7780–7781, 2003.

[6] P. Yang, M. Lü, D. Xü, D. Yuan, and G. Zhou, "Photoluminescence properties of ZnS nanoparticles co-doped with Pb^{2+} and Cu^{2+}," *Chemical Physics Letters*, vol. 336, no. 1-2, pp. 76–80, 2001.

[7] A. Agostiano, M. Catalano, M. L. Curri, M. Della Monica, L. Manna, and L. Vasanelli, "Synthesis and structural characterisation of CdS nanoparticles prepared in a four-components "water-in-oil" microemulsion," *Micron*, vol. 31, no. 3, pp. 253–258, 2000.

[8] A. Schroedter, H. Weller, R. Eritja, W. E. Ford, and J. M. Wessels, "Biofunctionalization of silica-coated CdTe and gold nanocrystals," *Nano Letters*, vol. 2, no. 12, pp. 1363–1367, 2002.

[9] J. McBride, J. Treadway, L. C. Feldman, S. J. Pennycook, and S. J. Rosenthal, "Structural basis for near unity quantum yield core/shell nanostructures," *Nano Letters*, vol. 6, no. 7, pp. 1496–1501, 2006.

[10] M. Bäumle, D. Stamou, J.-M. Segura, R. Hovius, and H. Vogel, "Highly fluorescent streptavidin-coated CdSe nanoparticles: preparation in water, characterization, and micropatterning," *Langmuir*, vol. 20, no. 10, pp. 3828–3831, 2004.

[11] X. Gao, L. Yang, J.A. Petros, J.W. Simons, and S. Nie, "In vivo molecular and cellular imaging with quantum dots," *Current Opinion in Biotechnology*, vol. 16, no. 1, pp. 63–72, 2005.

[12] A. P. Alivisatos, "Perspectives on the physical chemistry of semiconductor nanocrystals," *Journal of Physical Chemistry*, vol. 100, no. 1, pp. 13226–13239, 1996.

[13] C. B. Murray, D. J. Norris, and M. G. Bawendi, "Synthesis and characterization of nearly monodisperse CdE (E = S, Se, Te) semiconductor nanocrystallites," *Journal of the American Chemical Society*, vol. 115, no. 19, pp. 8706–8715, 1993.

[14] M. A. Hines and P. Guyot-Sionnest, "Synthesis and characterization of strongly luminescing ZnS-capped CdSe nanocrystals," *Journal of Physical Chemistry*, vol. 100, no. 2, pp. 468–471, 1996.

[15] W. Cai, D.-W. Shin, K. Chen, et al., "Peptide-labeled near-infrared quantum dots for imaging tumor vasculature in living subjects," *Nano Letters*, vol. 6, no. 4, pp. 669–676, 2006.

[16] M. Bruchez Jr., M. Moronne, P. Gin, S. Weiss, and A. P. Alivisatos, "Semiconductor nanocrystals as fluorescent biological labels," *Science*, vol. 281, no. 5385, pp. 2013–2016, 1998.

[17] W. C. W. Chan and S. Nie, "Quantum dot bioconjugates for ultrasensitive nonisotopic detection," *Science*, vol. 281, no. 5385, pp. 2016–2018, 1998.

[18] B. Dubertret, P. Skourides, D. J. Norris, V. Noireaux, A. H. Brivanlou, and A. Libchaber, "In vivo imaging of quantum dots encapsulated in phospholipid micelles," *Science*, vol. 298, no. 5599, pp. 1759–1762, 2002.

[19] D. Gerion, F. Pinaud, S. C. Williams, et al., "Synthesis and properties of biocompatible water-soluble silica-coated CdSe/ZnS semiconductor quantum dots," *Journal of Physical Chemistry B*, vol. 105, no. 37, pp. 8861–8871, 2001.

[20] T. M. Jovin, "Quantum dots finally come of age," *Nature Biotechnology*, vol. 21, no. 1, pp. 32–33, 2003.

[21] X. Gao, Y. Cui, R. M. Levenson, L. W. K. Chung, and S. Nie, "In vivo cancer targeting and imaging with semiconductor quantum dots," *Nature Biotechnology*, vol. 22, no. 8, pp. 969–976, 2004.

[22] X. Wu, H. Liu, J. Liu, et al., "Immunofluorescent labeling of cancer marker Her2 and other cellular targets with semiconductor quantum dots," *Nature Biotechnology*, vol. 21, no. 1, pp. 41–46, 2003.

[23] E. L. Bentzen, I. D. Tomlinson, J. N. Mason, et al., "Surface modification to reduce nonspecific binding of quantum dots in live cell assays," *Bioconjugate Chemistry*, vol. 16, no. 6, pp. 1488–1494, 2005.

[24] Z. Chunyang, M. Hui, D. Yao, J. Lei, C. Dieyan, and N. Shuming, "Quantum dot-labeled trichosanthin," *The Analyst*, vol. 125, no. 6, pp. 1029–1031, 2000.

[25] O. Minet, C. Dressler, and J. Beuthan, "Heat stress induced redistribution of fluorescent quantum dots in breast tumor cells," *Journal of Fluorescence*, vol. 14, no. 3, pp. 241–247, 2004.

[26] M. Howarth, K. Takao, Y. Hayashi, and A. Y. Ting, "Targeting quantum dots to surface proteins in living cells with biotin ligase," *Proceedings of the National Academy of Sciences of the United States of America*, vol. 102, no. 21, pp. 7583–7588, 2005.

[27] M. Howarth, D. J.-F. Chinnapen, K. Gerrow, et al., "A monovalent streptavidin with a single femtomolar biotin binding site," *Nature Methods*, vol. 3, no. 4, pp. 267–273, 2006.

[28] M.-V. Ehrensperger, C. Hanus, C. Vannier, A. Triller, and M. Dahan, "Multiple association states between glycine receptors and gephyrin identified by SPT analysis," *Biophysical Journal*, vol. 92, no. 10, pp. 3706–3718, 2007.

[29] I. L. Medintz and J. R. Deschamps, "Maltose-binding protein: a versatile platform for prototyping biosensing," *Current Opinion in Biotechnology*, vol. 17, no. 1, pp. 17–27, 2006.

[30] A. Månsson, M. Sundberg, M. Balaz, et al., "In vitro sliding of actin filaments labelled with single quantum dots," *Biochemical and Biophysical Research Communications*, vol. 314, no. 2, pp. 529–534, 2004.

[31] S. Le Gac, I. Vermes, and A. van den Berg, "Quantum dots based probes conjugated to annexin V for photostable apoptosis detection and imaging," *Nano Letters*, vol. 6, no. 9, pp. 1863–1869, 2006.

[32] M. E. Åkerman, W. C. W. Chan, P. Laakkonen, S. N. Bhatia, and E. Ruoslahti, "Nanocrystal targeting in vivo," *Proceedings of the National Academy of Sciences of the United States of America*, vol. 99, no. 20, pp. 12617–12621, 2002.

[33] D. S. Lidke, P. Nagy, R. Heintzmann, et al., "Quantum dot ligands provide new insights into erbB/HER receptor-mediated signal transduction," *Nature Biotechnology*, vol. 22, no. 2, pp. 198–203, 2004.

[34] I. D. Tomlinson, J. N. Mason, R. D. Blakely, and S. J. Rosenthal, "Peptide-conjugated quantum dots: imaging the angiotensin type 1 receptor in living cells," *Methods in Molecular Biology*, vol. 303, pp. 51–60, 2005.

[35] P. Alivisatos, "The use of nanocrystals in biological detection," *Nature Biotechnology*, vol. 22, no. 1, pp. 47–52, 2004.

[36] F. Patolsky, R. Gill, Y. Weizmann, T. Mokari, U. Banin, and I. Wiliner, "Lighting-up the dynamics of telomerization and DNA replication by CdSe-ZnS quantum dots," *Journal of the American Chemical Society*, vol. 125, no. 46, pp. 13918–13919, 2003.

[37] D. Gerion, W. J. Parak, S. C. Williams, D. Zanchet, C. M. Micheel, and A. P. Alivisatos, "Sorting fluorescent nanocrystals with DNA," *Journal of the American Chemical Society*, vol. 124, no. 24, pp. 7070–7074, 2002.

[38] Y. Xiao and P. E. Barker, "Semiconductor nanocrystal probes for human metaphase chromosomes," *Nucleic Acids Research*, vol. 32, no. 3, p. e28, 2004.

[39] W. J. Parak, D. Gerion, D. Zanchet, et al., "Conjugation of DNA to silanized colloidal semiconductor nanocrystalline quantum dots," *Chemistry of Materials*, vol. 14, no. 5, pp. 2113–2119, 2002.

[40] C. Srinivasan, J. Lee, F. Papadimitrakopoulos, L. K. Silbart, M. Zhao, and D. J. Burgess, "Labeling and intracellular tracking of functionally active plasmid DNA with semiconductor quantum dots," *Molecular Therapy*, vol. 14, no. 2, pp. 192–201, 2006.

[41] E. Tholouli, J. A. Hoyland, D. Di Vizio, et al., "Imaging of multiple mRNA targets using quantum dot based *in situ* hybridization and spectral deconvolution in clinical biopsies," *Biochemical and Biophysical Research Communications*, vol. 348, no. 2, pp. 628–636, 2006.

[42] C.-Y. Zhang, H.-C. Yeh, M. T. Kuroki, and T.-H. Wang, "Single-quantum-dot-based DNA nanosensor," *Nature Materials*, vol. 4, no. 11, pp. 826–831, 2005.

[43] A. Fu, C. M. Micheel, J. Cha, H. Chang, H. Yang, and A. P. Alivisatos, "Discrete nanostructures of quantum dots/Au with DNA," *Journal of the American Chemical Society*, vol. 126, no. 35, pp. 10832–10833, 2004.

[44] W. B. Tan, S. Jiang, and Y. Zhang, "Quantum-dot based nanoparticles for targeted silencing of HER2/neu gene via RNA interference," *Biomaterials*, vol. 28, no. 8, pp. 1565–1571, 2007.

[45] R. Chakrabarti and A. M. Klibanov, "Nanocrystals modified with peptide nucleic acids (PNAs) for selective self-assembly and DNA detection," *Journal of the American Chemical Society*, vol. 125, no. 41, pp. 12531–12540, 2003.

[46] S. Bryde, I. Grunwald, A. Hammer, et al., "Tumor necrosis factor (TNF)-functionalized nanostructured particles for the stimulation of membrane TNF-specific cell responses," *Bioconjugate Chemistry*, vol. 16, no. 6, pp. 1459–1467, 2005.

[47] M. Manchester and P. Singh, "Virus-based nanoparticles (VNPs): platform technologies for diagnostic imaging," *Advanced Drug Delivery Reviews*, vol. 58, no. 14, pp. 1505–1522, 2006.

[48] L. Dyadyusha, H. Yin, S. Jaiswal, et al., "Quenching of CdSe quantum dot emission, a new approach for biosensing," *Chemical Communications*, no. 25, pp. 3201–3203, 2005.

[49] E. R. Goldman, A. R. Clapp, G. P. Anderson, et al., "Multiplexed toxin analysis using four colors of quantum dot fluororeagents," *Analytical Chemistry*, vol. 76, no. 3, pp. 684–688, 2004.

[50] M. Dahan, S. Lévi, C. Luccardini, P. Rostaing, B. Riveau, and A. Triller, "Diffusion dynamics of glycine receptors revealed by single-quantum dot tracking," *Science*, vol. 302, no. 5644, pp. 442–445, 2003.

[51] J. N. Mason, H. Farmer, I. D. Tomlinson, et al., "Novel fluorescence-based approaches for the study of biogenic amine transporter localization, activity, and regulation," *Journal of Neuroscience Methods*, vol. 143, no. 1, pp. 3–25, 2005.

[52] B. Ballou, B. C. Lagerholm, L. A. Ernst, M. P. Bruchez, and A. S. Waggoner, "Noninvasive imaging of quantum dots in mice," *Bioconjugate Chemistry*, vol. 15, no. 1, pp. 79–86, 2004.

[53] S. Kim, Y. T. Lim, E. G. Soltesz, et al., "Near-infrared fluorescent type II quantum dots for sentinel lymph node mapping," *Nature Biotechnology*, vol. 22, no. 1, pp. 93–97, 2004.

[54] C. Bouzigues, M. Morel, A. Triller, and M. Dahan, "Asymmetric redistribution of GABA receptors during GABA gradient sensing by nerve growth cones analyzed by single quantum dot imaging," *Proceedings of the National Academy of Sciences of the United States of America*, vol. 104, no. 27, pp. 11251–11256, 2007.

[55] S. J. Rosenthal, I. D. Tomlinson, E. M. Adkins, et al., "Targeting cell surface receptors with ligand-conjugated nanocrystals,"

Journal of the American Chemical Society, vol. 124, no. 17, pp. 4586–4594, 2002.

[56] I. D. Tomlinson, A. P. Gies, P. J. Gresch, et al., "Universal polyethylene glycol linkers for attaching receptor ligands to quantum dots," *Bioorganic & Medicinal Chemistry Letters*, vol. 16, no. 24, pp. 6262–6266, 2006.

[57] I. D. Tomlinson, J. L. Grey, and S. J. Rosenthal, "A synthesis of 6-(2,5-dimethoxy-4-(2-aminopropyl)phenyl)-hexylthiol. A ligand for conjugation with fluorescent cadmium selenide/zinc sulfide core/shell nanocrystals and biological imaging," *Molecules*, vol. 7, no. 11, pp. 777–790, 2002.

[58] I. D. Tomlinson, J. Mason, J. N. Burton, R. Blakely, and S. J. Rosenthal, "The design and synthesis of novel derivatives of the dopamine uptake inhibitors GBR 12909 and GBR 12935. High-affinity dopaminergic ligands for conjugation with highly fluorescent cadmium selenide/zinc sulfide core/shell nanocrystals," *Tetrahedron*, vol. 59, no. 40, pp. 8035–8047, 2003.

[59] I. D. Tomlinson, J. N. Mason, R. D. Blakely, and S. J. Rosenthal, "Inhibitors of the serotonin transporter protein (SERT): the design and synthesis of biotinylated derivatives of 3-(1,2,3,6-tetrahydro-pyridin-4-yl)-1H- indoles. High-affinity serotonergic ligands for conjugation with quantum dots," *Bioorganic & Medicinal Chemistry Letters*, vol. 15, no. 23, pp. 5307–5310, 2005.

[60] I. D. Tomlinson, J. N. Mason, R. D. Blakely, and S. J. Rosenthal, "High affinity inhibitors of the dopamine transporter (DAT): novel biotinylated ligands for conjugation to quantum dots," *Bioorganic & Medicinal Chemistry Letters*, vol. 16, no. 17, pp. 4664–4667, 2006.

[61] J. N. Mason, I. D. Tomlinson, S. J. Rosenthal, and R. D. Blakely, "Labeling cell-surface proteins via antibody quantum dot streptavidin conjugates," *Methods in Molecular Biology*, vol. 303, pp. 35–50, 2005.

[62] I. D. Tomlinson, T. Kippeny, L. Swafford, N. H. Siddiqui, and S. J. Rosenthal, "Novel polyethylene glycol derivatives of melatonin and serotonin. Ligands for conjugation to fluorescent cadmium selenide/zinc sulfide core shell nanocrystals," *Journal of Chemical Research*, vol. 2002, no. 5, pp. 203–204, 2002.

[63] A. Wolcott, D. Gerion, M. Visconte, et al., "Silica-coated CdTe quantum dots functionalized with thiols for bioconjugation to IgG proteins," *Journal of Physical Chemistry B*, vol. 110, no. 11, pp. 5779–5789, 2006.

[64] E. R. Goldman, G. P. Anderson, P. T. Tran, H. Mattoussi, P. T. Charles, and J. M. Mauro, "Conjugation of luminescent quantum dots with antibodies using an engineered adaptor protein to provide new reagents for fluoroimmunoassays," *Analytical Chemistry*, vol. 74, no. 4, pp. 841–847, 2002.

[65] H. A. Gussin, I. D. Tomlinson, D. M. Little, et al., "Binding of muscimol-conjugated quantum dots to $GABA_C$ receptors," *Journal of the American Chemical Society*, vol. 128, no. 49, pp. 15701–15713, 2006.

[66] M. Frey and V. Jäger, "Synthesis of *N*-substituted muscimol derivatives including *N*-glycylmuscimol," *Synthesis*, vol. 1985, no. 12, pp. 1100–1104, 1985.

[67] H. Qian, J. E. Dowling, and H. Ripps, "Molecular and pharmacological properties of GABA-ρ subunits from white perch retina," *Journal of Neurobiology*, vol. 37, no. 2, pp. 305–320, 1998.

[68] T. Q. Vu, S. Chowdhury, N. J. Muni, H. Qian, R. F. Standaert, and D. R. Pepperberg, "Activation of membrane receptors by a neurotransmitter conjugate designed for surface attachment," *Biomaterials*, vol. 26, no. 14, pp. 1895–1903, 2005.